

Comb-Shaped Poly(arylene ether sulfone)s as Proton Exchange Membranes[†]

Dae Sik Kim, Gilles P. Robertson, and Michael D. Guiver*

*Institute for Chemical Process and Environmental Technology, National Research Council,
1200 Montreal Road, Ottawa, Ontario K1A 0R6, Canada*

Received December 6, 2007; Revised Manuscript Received January 11, 2008

ABSTRACT: A new sulfonated side-chain grafting unit containing two or four sulfonic acid groups was synthesized using sulfonated 4-fluorobenzophenone (FBP) and 1,1-bis(4-hydroxyphenyl)-1,4-((4-fluorophenyl)thio)phenyl-2,2,2-trifluoroethane (3FBPT). A conventional aromatic nucleophilic substitution (S_NAr) was used for copolymerization of poly(arylene ether sulfone) containing a methoxy group. After converting the methoxy group to the reactive hydroxyl group, this functionalized copolymer was reacted to graft the sulfonated side chains to make the comb-shaped sulfonated poly(arylene ether sulfone) copolymers. All the polymers were characterized by 1H NMR, thermogravimetric analysis (TGA), the water uptake, and proton and methanol transport for fuel cell applications. These comb-shaped sulfonated polymers had good properties as polyelectrolyte membrane materials. The comb-shaped copolymers with two or four sulfonic acid groups show high proton conductivity in the range of 34–147 and 63–125 mS/cm, respectively. The methanol permeabilities of these copolymers were in the range of 8.2×10^{-7} – 5.6×10^{-8} cm²/s. A combination of high proton conductivities, low water uptake, and low methanol permeabilities for some of the comb-shaped copolymers indicated that they are good candidate materials for proton exchange membrane in fuel cell applications.

Introduction

Extensive efforts have been made to develop alternative hydrocarbon-based polymer electrolyte membranes to overcome the drawbacks of the current widely used perfluorosulfonic acid Nafion.^{1,2} As a class of high-performance engineering thermoplastic materials, poly(arylene ether)s have high glass transition temperatures, high thermal stabilities, good mechanical properties and excellent resistance to hydrolysis and oxidation. Functionalized poly(arylene ether)s may find many applications as membrane materials for gas separation, water desalination, and for fuel cells as proton exchange membrane (PEM).¹ Sulfonated derivatives of poly(ether sulfone) (SPES),^{3–5} polyimide (SPI),^{6–8} polyimidazole,⁹ poly(aryl ether),^{10,11} polyphe-nylene,^{12,13} and poly(phenylquinoxaline)¹⁴ are among those being investigated as potential PEMs. Alternatively, sulfonated polymers can be prepared by direct polymerization using sulfonated monomer,^{15–17} or post-sulfonation.¹⁸ The majority of this work is based on polyaromatic-based condensation polymers that contain the sulfonic acid groups located along the polymer backbone (Scheme 1a). Generally, these polymers show suitable conductivities only at high ion-exchange capacities (IEC)s, resulting in extensive water uptake above a critical temperature (percolation threshold), or a dramatic loss of mechanical properties that are unsuitable for practical PEM applications. Kreuer et al.¹⁹ reported that these sulfonated polymers are unable to form defined hydrophilic domains, as the rigid polyaromatic backbone prevents continuous ionic clustering from occurring. One promising way to enhance properties in terms of PEM performance is to distinctly separate the hydrophilic sulfonic acid group regions from the hydrophobic polymer main chain by locating the sulfonic acid groups on side chains grafted onto the polymer main chain.²⁰ Ding et al. reported the properties of graft polymers comprising graft

chains of a macromonomer poly(sodium styrenesulfonate) and a polystyrene backbone.²¹ If flexible pendant side chains linking the polymer main chain and the sulfonic acid groups exist in the polymer structure, nanophase separation between hydrophilic and hydrophobic domains may be improved.²² Nafion is a statistical copolymer comprising a highly hydrophobic perfluorinated backbone that contains a number of short, flexible pendant side chains with single strongly hydrophilic sulfonic acid groups. The structure of Nafion produces nanophase-separated morphology of membranes, and thus they show excellent thermal, mechanical, and electrochemical properties. The flexibility of the side chain of Nafion allows for the aggregation of the superacid fluoroalkyl sulfonic sites into channels, which conduct protons well. However, the proton conductivity of Nafion is reduced above 100 °C due to morphological relaxations.²⁰

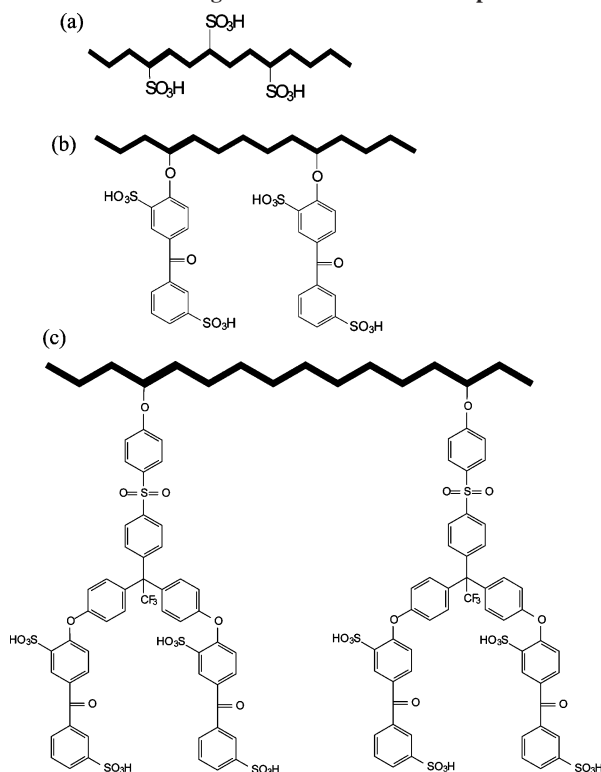
Jannasch and co-workers reported a sulfophenoxybenzoyl polysulfone and sulfonaphthoxybenzoyl polysulfone that was prepared by attaching pendant sulfonated aromatic side chains to polysulfone, showing proton conductivities of 11–32 mS/cm at 120 °C.²² In our previous report, a series of highly fluorinated polyaromatic-based comb-shaped copolymers were prepared that display advantageous conductivity and membrane hydrodynamic properties as compared to most sulfonated arylene main-chain polymers.²³ Einsla et al. reported that sulfonated poly(arylene ether sulfone) copolymers with pendant sulfonic acid groups were prepared using barium pentafluorobenzene-sulfonate and 4-nitrobenzenesulfonyl chloride, showing lower proton conductivity (1–8 mS/cm).²⁰

Herein, we report on a series of wholly aromatic comb-shaped copolymers wherein the sulfonic acid sites are on linear as branched pendent chains. Poly(arylene ether sulfone) copolymers containing methoxy groups were first prepared, and then the methoxy groups were converted to reactive hydroxyl groups, similar to a procedure reported previously.²⁰ Hydroxyl group with two different activated side chains provided copolymers with either linear (two sulfonic acid groups) or branched (four

[†] NRCC Publication No. 49131.

* Corresponding author: Tel +1 613 993 9753; Fax +1 613 991 2384; e-mail Michael.Guiver@nrc-cnrc.gc.ca.

Scheme 1. Representations of (a) a Typical Polyaromatic-based PEM Displaying a Rigid and Sulfonated Hydrocarbon Backbone, (b) Our Materials Based on Rigid Polyaromatic Backbone with Pendant Side Chains Containing Two Sulfonic Acid Groups, and (c) with Branched Pendant Side Chain Containing Four Sulfonic Acid Groups



sulfonic acid groups) side chains. Unlike previous copolymers graft with less stable polystyrene, the main chain of the present copolymer series is comprised of thermally and chemically stable repeat units, and the side chain segments containing the ionic groups are also stable and flexible, allowing the formation of ionic domains (Scheme 1b,c). The present work demonstrates the feasibility and success of this synthetic approach to produce high molecular weight wholly aromatic comb-shaped copolymers with sulfonated side chains. The resulting copolymer properties related to PEM materials for fuel cell applications were also evaluated thoroughly.

Experimental Section

Materials. 4,4'-Difluorodiphenylsulfone (DFS), 4,4'-bisphenol (BP), methoxyhydroquinone (Me-HQ), and 4-fluorobenzophenone (FBP) were purchased from Sigma-Aldrich Ltd. 4-Fluoro-2,2,2-trifluoroacetophenone (F3FAP), trifluoromethanesulfonic acid (triflic acid), and 4-fluorothiophenol (FTP) were purchased from Oakwood Products Inc. and used as received. 4,4'-Biphenol (Sigma-Aldrich) was purified by crystallization from ethanol, and methoxyhydroquinone was dried at room temperature under vacuum before use. Dimethyl sulfoxide (DMSO) and *N*-methyl-2-pyrrolidone (NMP) (Sigma-Aldrich) was vacuum-distilled prior to use. All other chemicals were reagent grade from Sigma-Aldrich and were used as received.

Sulfonated Monomer 1-a (Sulfonated Fluorobenzophenone (S-FBP)). A mixture of 4-fluorobenzophenone (FBP) (20 g) and 30% fuming sulfuric acid (31 mL, $\text{FBP}:\text{SO}_3 = 0.1 \text{ mol}:50 \text{ mL}$) was heated at 110°C for 20 h. The solution was cooled and poured into ice water (250 mL). NaCl (113 g) was added, which produced a white precipitate identified as the disodium salt of S-FBP. The powder was filtered and redissolved in 250 mL of water, and then the pH was increased to 6–7 by the addition of aqueous 2 N NaOH. An excess of NaCl was added to salt out the sodium form of

disulfonated monomer. The crude product was recrystallized from a mixture of methanol and water (7:3 vol %).

Synthesis of 1,1-Bis(4-hydroxyphenyl)-1-(4-((4-fluorophenyl)-thio)phenyl)-2,2,2-trifluoroethane (3FBPT, 1-b). 3FBPT (1-b) monomer was synthesized according to the method in the literature.²⁴ Yield: 94%. ^1H NMR (DMSO- d_6 , ppm): 9.63 (s, 2H), 7.52 (dd, 2H), 7.29 (t, 2H), 7.18 (d, $J = 8.8 \text{ Hz}$, 2H), 7.00 (d, $J = 8.8 \text{ Hz}$, 2H), 6.80 (d, $J = 8.8 \text{ Hz}$, 4H), 6.74 (d, $J = 8.8 \text{ Hz}$, 4H). ^{19}F NMR (DMSO- d_6 , ppm): -57.9 (s, 3F), -112.5 (m, 1F). MS (m/z): 488.2 ($[\text{M} + \text{NH}_4]^+$). FT-IR (diamond plate, cm^{-1}): 3400 ($-\text{OH}$), 820 (Ar).

Synthesis and Oxidation of Sulfonated Graft Pendant Side Chain 1-c and 1-d. 4 mmol of S-FBP (1-a), 2 mmol of 3FBPT (1-b), and 3 mmol of K_2CO_3 were added into a three-neck flask equipped with a magnetic stirrer, a Dean–Stark trap, and an argon gas inlet. Then, 10 mL of DMSO and 10 mL of toluene were charged into the reaction flask under an argon atmosphere. The reaction mixture was heated to 150°C . After dehydration and removal of toluene, the reaction temperature was increased to about 170°C for 6 h. The mixture was cooled to room temperature and coagulated into a large excess of chloroform with vigorous stirring. The resulting white powder sulfonated graft unit (1-c) was washed thoroughly with water several times and dried under vacuum at 100°C for 24 h. Yield 95%.

In a typical oxidation procedure, sulfonated monomer (1-c) (3.0 g) was added into 130 mL of formic acid, and 13 mL of 30% hydrogen peroxide was added dropwise at 40°C . The heterogeneous dispersion was stirred vigorously for 1.5 h. The solvent was removed by a rotary evaporator. Yield 80%.

The syntheses of S-FBP (1-a), 3FBPT (1-b), and sulfonated branched graft unit (1-d) are illustrated in Scheme 2.

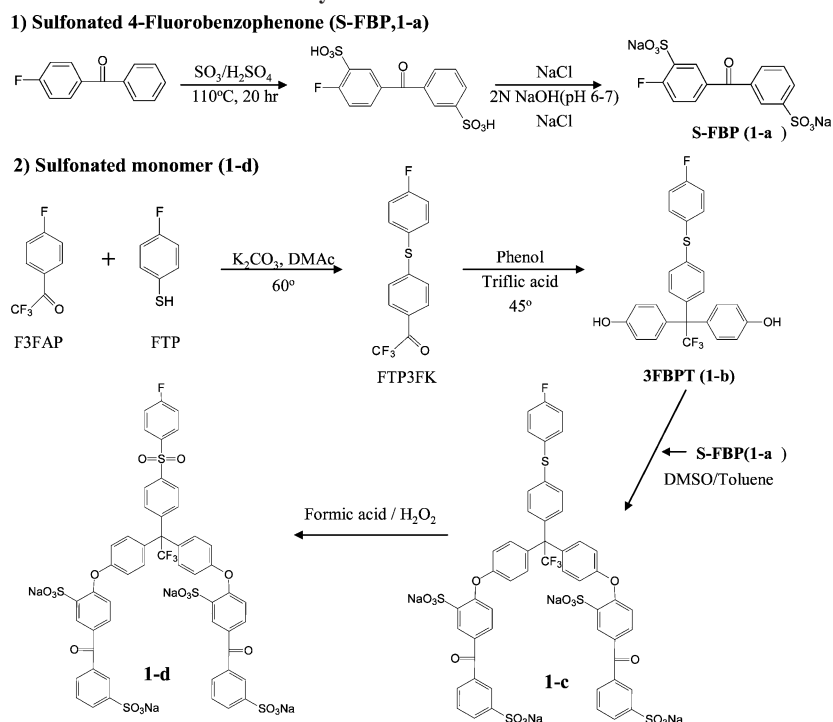
Copolymerization of Poly(arylene ether sulfone)s Containing Methoxy Group (PAES-xx-Me). A typical synthetic procedure, illustrated by the preparation of PAES-50-Me copolymers (Me-HQ/BP = 50/50), is described as follows.²⁰ In a typical reaction, 10 mmol of DFS, 5 mmol of Me-HQ, 5 mmol of BP, and 12 mmol of K_2CO_3 were added into a three-neck flask equipped with a magnetic stirrer, a Dean–Stark trap, and an argon gas inlet. Then, 15 mL of NMP and 15 mL of toluene were charged into the reaction flask under an argon atmosphere. The reaction mixture was heated to 145°C . After dehydration and removal of toluene, the reaction temperature was increased to about 170°C . When the increase of the solution viscosity became obvious, the mixture was cooled to room temperature and coagulated into a large excess of deionized water with vigorous stirring. The resulting fibrous copolymer was washed thoroughly with water or ethanol several times and dried under vacuum at 100°C for 24 h. The copolymer was denoted PAES-50-Me, where n (50) refers to the Me-HQ molar content. Yield: 97%.

Conversion of Methoxy (PAES-xx-Me) to Hydroxyl Group (PAES-xx-OH). PAES-50-Me (1.0 g) was dissolved into 20 mL of chloroform in a 100 mL, three-neck flask equipped with a magnetic stirrer and an argon gas inlet. BBr_3 (1 mL) was mixed with chloroform (10 mL). BBr_3 solution was added dropwise to the PAES-50-Me solution at room temperature. After 8 h, the copolymer was filtered and washed with methanol and deionized water. The resulting copolymer (PAES-50-OH) was dried under vacuum at 120°C for 24 h. Yield: 98%.

Preparation of Sulfonated Copolymer, S2-PAES-50 and S4-PAES-50. The copolymers are denoted as $\text{S}_x\text{-PAEEN-yy}$, where x refers to the number of sulfonic acid groups in the side chain and yy is the mole percent of the pendant group unit relative to DFS. For example, S2-PAES-50 describes the poly(arylene ether sulfone)s copolymer that incorporates 50 mol % of Me-HQ and in grafted with S-FBP (that has two sulfonic acid groups).

HO-PAES-50 (0.7548 g, 1.0 mmol of OH group), S-FBP (1-a, 0.808 g, 2.0 mmol) for S2-PAES-50, or sulfonated monomer (1-d, 2.54 g, 2.0 mmol) for S4-PAES-50, K_2CO_3 (0.21 g 1.5 mmol), 20 mL of DMAc, and 10 mL of toluene were added into a argon flushed reactor which was equipped with a Dean–Stark trap. The reaction mixture was heated to 145°C . After dehydration and

Scheme 2. Synthesis of Sulfonated Monomers



removal of toluene, the reaction temperature was increased to about 170 °C for 20 h. The mixture was coagulated into a large excess of HCl (5 wt %) solution with vigorous stirring and washed with water. The resulting copolymers (S2-PAES-50, S4-PAES-50) were dried under vacuum at 100 °C for 24 h. Yield: 98% and 97%, respectively.

Measurements. NMR spectra were recorded in DMSO- d_6 using a Varian Unity Inova spectrometer at a resonance frequency of 399.96 MHz for ^1H . Signals from DMSO- d_6 were used as the reference for ^1H (2.50 ppm).

The molecular weights of polymers were determined by gel permeation chromatography (GPC) using a Waters 515 HPLC pump, coupled with a Waters 410 differential refractometer detector and a Waters 996 photodiode array detector. THF was used as the eluant and the μ -Styragel columns were calibrated by polystyrene standards.

The thermal gravimetric analysis (TGA) was performed using a TA Instruments TGA 2950 at a heating rate of 10 °C/min under a nitrogen atmosphere (50 mL/min).

TEM Samples were stained by immersing films in lead acetate aqueous solution (0.5 M), thoroughly washed with water, and dried at room temperature for 24 h. The polymer samples were embedded in polystyrene. Specimen microtome was performed using Reichert-Jung UltraCut E. A sample slice was placed onto a 300 mesh carbon-coated holey TEM copper grid and was dried in vacuum. The dried grid was then loaded into a double tilt sample holder. The sample was thus examined with a Philips CM20 STEM equipped with a Gatan UltraScan 1000 CCD camera combined with a Digital Micrograph Software (dm3.4) and an energy-dispersive X-ray spectrometer: INCA Energy TEM 200. TEM images were taken at 120 kV.

The proton conductivities of the membranes were estimated from ac impedance spectroscopy data using a Solartron 1260 gain phase analyzer. Each specimen was placed into water mounted in a cell that was temperature controlled and open to the air by a pinhole. Each end of the membrane strip was clamped in a frame between two platinum wire electrodes. The conductivity (σ) of the samples in the longitudinal direction was calculated, using the relationship $\sigma = L/(RdW)$, where L is the distance between the electrodes; d and W are the thickness and width of the sample stripe, respectively. R was derived from the low intersect of the high-frequency semicircle on a complex impedance plane with the Re (Z) axis.

Methanol permeability was measured using a simple two-compartment glass diffusion cell. A membrane (2 cm \times 2 cm) was placed between two silicone rubber gaskets and with the two compartments clamped together around the gaskets. The active area of the membrane was 1.757 cm². Compartment A was filled with 100 mL of 10% v/v (2.47 M) methanol with an internal standard of 0.2% v/v (0.022 M) 1-butanol in aqueous solution. Compartment B was filled with 100 mL of 0.2% v/v 1-butanol solution. The diffusion cell was placed in a water bath held at 30 °C, and each compartment was stirred by a separate stir plate to ensure uniform stirring. Methanol concentrations were determined by ^1H NMR spectroscopy.

Characterization Methods. The density of membrane was measured from a known membrane dimension and weight after drying at 75 °C for 2 h. Water uptake was measured after drying the membrane in acid form at 100 °C under vacuum overnight. The dried membrane was immersed in water at 30 °C and periodically weighed on an analytical balance until a constant water uptake weight was obtained. Then, the volume-based water uptake (WU) was obtained. A volume-based IEC (IEC_V) was obtained by multiplying the membrane density by the IEC_W values which were estimated from the copolymer structure. This calculation resulted in IEC_V (dry) based on the dry membrane density. An IEC_V (wet) was then calculated based on membrane water uptake.

Results and Discussion

Graft Side-Chain Synthesis. High yields of S-FBP monomers were prepared via electrophilic aromatic substitution on FBP in fuming sulfuric acid with the reaction conditions as depicted in Scheme 2. The molecular structure of S-FBP (**1-a**) was confirmed using ^1H NMR spectroscopy. As shown in Figure 1b, S-FBP with one $-\text{SO}_3\text{Na}$ group was obtained after 6 h reaction time. The S-FBP with two $-\text{SO}_3\text{Na}$ groups was obtained clearly after an extended reaction time (20 h). In the ^1H NMR spectrum of S-FBP (Figure 1b,c), the proton peak ortho to sulfonate group ($3' + 2$) appeared at high frequency (7.91–7.93 and 8.05–8.10 ppm), which is attributed to two electron-withdrawing groups. This result indicates that two sulfonic acid groups were attached at the FBP monomer.

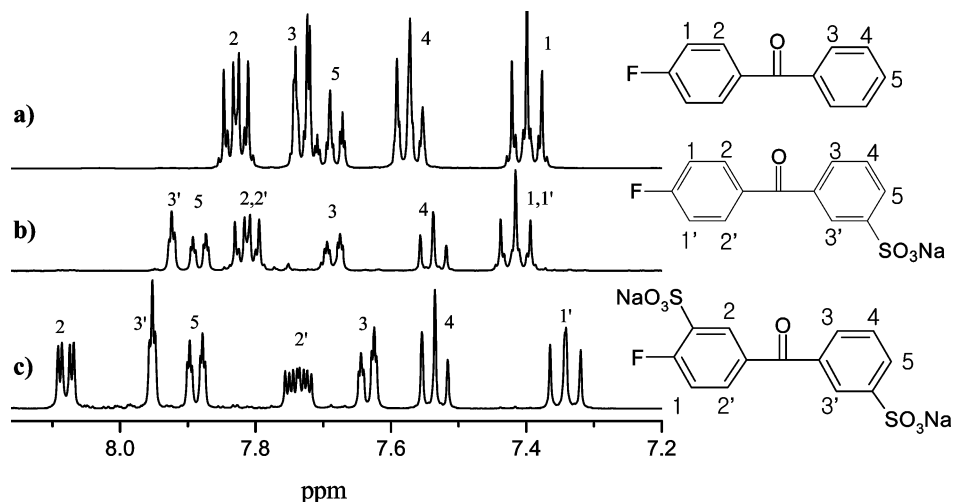


Figure 1. ^1H NMR of sulfonated monomer (1-a).

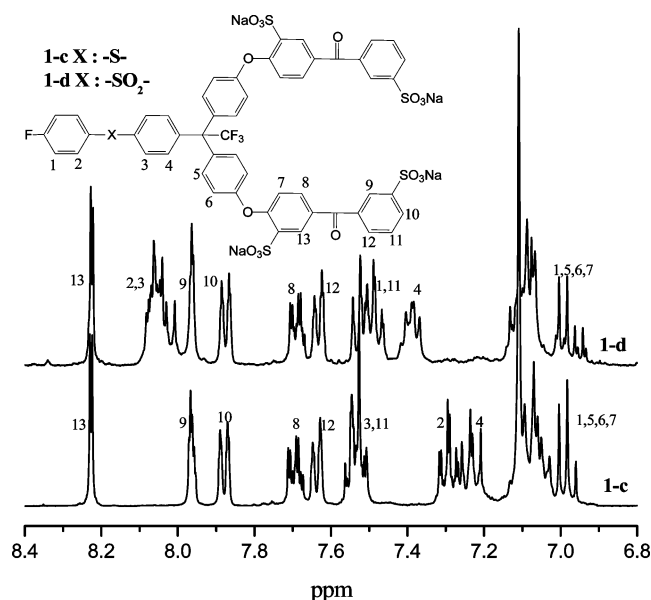


Figure 2. ^1H NMR of sulfonated monomer (1-c and 1-d).

As shown in Scheme 2 (2), the synthesis of monomer 3FBPT (1-b) comprises two steps. The activated fluorine of F3FAP was reacted with FTP. The resulting FTP3FK was then condensed with 2 mol of phenol to produce the bisphenol (3FBPT).²⁵ The overall yield of the two step reaction was above 90%, and the proposed structure was confirmed by ^1H NMR spectra. The 3FBPT (1-b) monomer was reacted with S-FBP (1-a) to make the sulfonated branched unit to sulfone 1-c. The 4-fluorophenyl thioether groups of sulfonated unit 1-c were oxidized so as to activate the fluoro group using hydrogen peroxide in heterogeneous peroxide polymer formic acid suspension for reaction with $-\text{OH}$ group of polymer main chain.²⁶ ^1H NMR confirms the synthesis of sulfonated monomer 1-c and that complete oxidation occurred. In the ^1H NMR spectra of 1-c and 1-d (Figures 2), the proton peak (9 and 13) ortho to sulfonate group appeared at high frequency 7.94–7.98 and 8.21–8.24 ppm, respectively. The ortho-sulfonyl protons appear at higher frequencies due to deshielding from the sulfone groups.

Copolymerization of Poly(arylene ether sulfone)s (PAES-xx-Me, PAES-xx-OH). Poly(arylene ether sulfone)s containing pendant methoxy groups (PAES-xx-Me, xx: mole ratio (%) of Me-HQ) were synthesized by polycondensation using various feed ratios of Me-HQ/BP, so that polymers with different molar percentage of pendant group were obtained (Scheme 3).

The polymerization reactions proceeded smoothly, and no cross-linking was evident when the temperature and reaction time were well controlled by an oil bath (less than 170 $^\circ\text{C}$) and less than 10 h because the methoxy groups are not reactive under these conditions, so high molecular weights ($M_n > 50\,000$ g/mol) were obtained. The data of molecular weight, polydispersity index, and intrinsic viscosity are listed in Table 1. It was found that higher temperature (above 170 $^\circ\text{C}$) or longer reaction time (longer than 10 h) would lead to some cross-linked gel-like polymer, indicating that the methoxy groups are reactive under these conditions using K_2CO_3 .

The conversion of the $-\text{OCH}_3$ groups to reactive $-\text{OH}$ groups using BBr_3 was conducted in Chloroform.²⁰ The PAES-xx-Me copolymers were soluble in chlorinated solvents. However, the PAES-xx-OH copolymers were not soluble in chloroform due to the polar nature of the $-\text{OH}$ group. Therefore, the PAES-xx-Me copolymer was converted to PAES-xx-OH and the converted copolymer precipitated from chloroform solvent. Table 1 showed the η and molecular weight of PAES-xx-OH copolymer, showing η of PAES-xx-OH was higher than the PAES-xx-Me copolymer due to hydrogen bonding of the $-\text{OH}$ groups.²⁰ The conversion of $-\text{OCH}_3$ groups to $-\text{OH}$ groups was confirmed by ^1H NMR. The protons of $-\text{OCH}_3$ groups at 3.6 ppm disappeared, and the proton of $-\text{OH}$ groups appeared at 10 ppm as shown in Figure 3a.

Copolymerization of Sulfonated Poly(arylene ether sulfone)s (S2-PAES-xx, S4-PAES-xx). To demonstrate the reactivity of the $-\text{OH}$ as a grafting side on PAES-xx-OH and prepare the sulfonated polymer, PAES-xx-OH was further reacted with an activated fluorine atom of sulfonated monomer (1-a and 1-d) by nucleophilic substitution. As shown in Figure 3b, a preliminary ^1H NMR study showed that the complete disappearance of the proton of the $-\text{OH}$ group at 10 ppm was observed, and the proton ortho to sulfonate group of S2-PAES-50 and S4-PAES-50 copolymer appeared at 8.15–8.12 and 8.24–8.20 ppm, respectively. All of the sulfonated polymers were readily soluble in DMAc and formed transparent, flexible, and tough membranes after solution casting, which implies that no cross-linking or degradation occurred during the side-group attachment reaction. Further evidence comes from the η measurement; sulfonated polymer shows a little bit higher inherent viscosity because of the attachment of sulfonated side chain, which gives a stronger interaction between polymer chains, and this results agrees well with previous reports.¹

Scheme 3. Synthesis of PAES-xx-Me, PAES-xx-OH, and Sulfonated Polymers

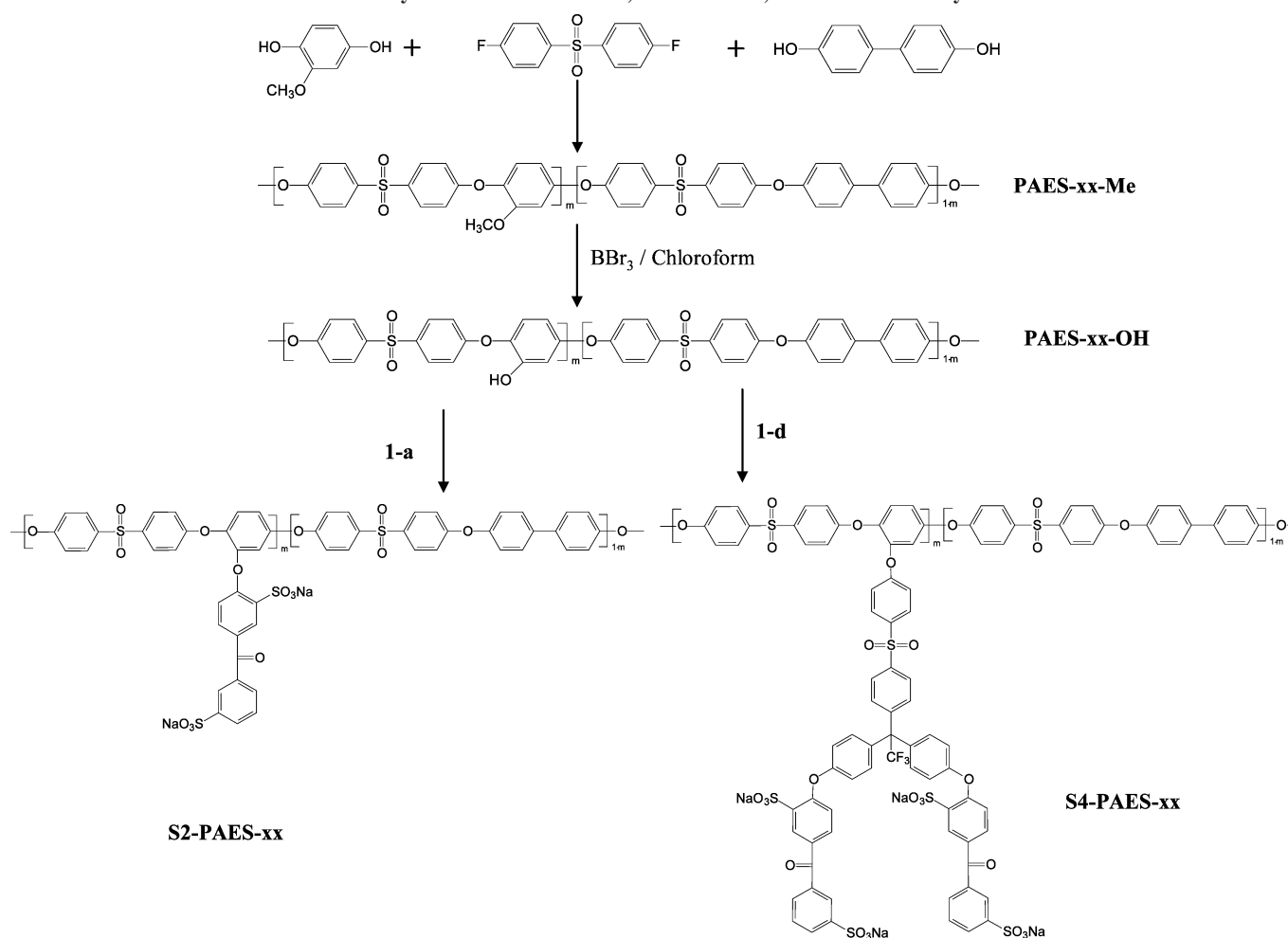


Table 1. Characterization of Polymers

copolymer	$[\eta]^a$ (dL/g)	mol wt ^b ($\times 10^3$ mol/g)		PDI	$T_{d(5\%)}^c$ (°C)	tensile strength (MPa)	Young's modulus (GPa)	elongation at break (%)
		M_n	M_w					
PAES-30-Me	1.32	63.1	69.9	1.10	419.4	50	1.34	8.8
PAES-40-Me	1.35	72.0	107	1.49	415.6	64	1.40	12.2
PAES-50-Me	1.41	65.7	82.9	1.26	410.8	56	0.78	18.5
PAES-60-Me	1.32	46.2	52.2	1.12	407.5	52	0.98	11.5
PAES-30-OH	1.42	42.0	48.9	1.16	416.2	51	1.46	10.7
PAES-40-OH	1.45	54.7	64.7	1.18	410.2	63	1.25	27.0
PAES-50-OH	1.51	57.2	66.9	1.16	407.2	58	0.82	23.0
PAES-60-OH	1.41	45.3	51.2	1.13	405.5	57	1.02	17.2
S2-PAES-30	1.58				354.6	49 (37) ^d	1.3 (0.84)	8.3 (21.6)
S2-PAES-40	1.62				364.6	47 (39)	1.1 (0.93)	9.3 (31)
S2-PAES-50	1.68				345.3	40 (38)	0.97 (0.75)	10.5 (12.1)
S2-PAES-60	1.69				338.5	48 (35)	0.88 (0.71)	10.0 (36)
S4-PAES-30	1.65				366.5	48 (33)	0.95 (0.79)	9.5 (21)
S4-PAES-40	1.68				342.5	24 (30)	0.75 (0.84)	4.0 (15.2)
S4-PAES-50	1.72				337.8	21 (32)	0.74 (0.65)	4.7 (13.1)

^a Measured at 25 °C in DMAc measured by GPC using THF as solvent. ^b The low molecular weight cyclic polymer peak was not included for calculation of M_n , M_w , and PDI. ^c 5% weight loss temperature in N₂ gas (acid form membrane). ^d Wet samples.

Thermal and Mechanical Properties. All the unsulfonated copolymers showed excellent thermal stability judged by TGA curves. 5% weight loss temperatures of copolymer are listed in Table 1. Both PAES-xx-Me and PAES-xx-OH copolymers showed similar TGA results ($T_{d(5\%)}$), indicating that the $-\text{OCH}_3$ group and $-\text{OH}$ group substitution did not influence the thermal stability. After attachment of sulfonated side chain, the thermal decomposition temperatures decreased because of the introduction of sulfonic acid groups as shown in Figure 4. The first

decomposition stage around 250–350 °C was possibly associated with the loss of bound water and degradation of the sulfonic acid groups, and the second decomposition stage around 500 °C was likely related to the degradation of the main and side chains.

Good mechanical properties of the PEMs in both wet and dry states are one of the demands for DMFC applications. The mechanical properties of the unsulfonated membranes and comb-shaped sulfonated polymers are listed in Table 1. The unsul-

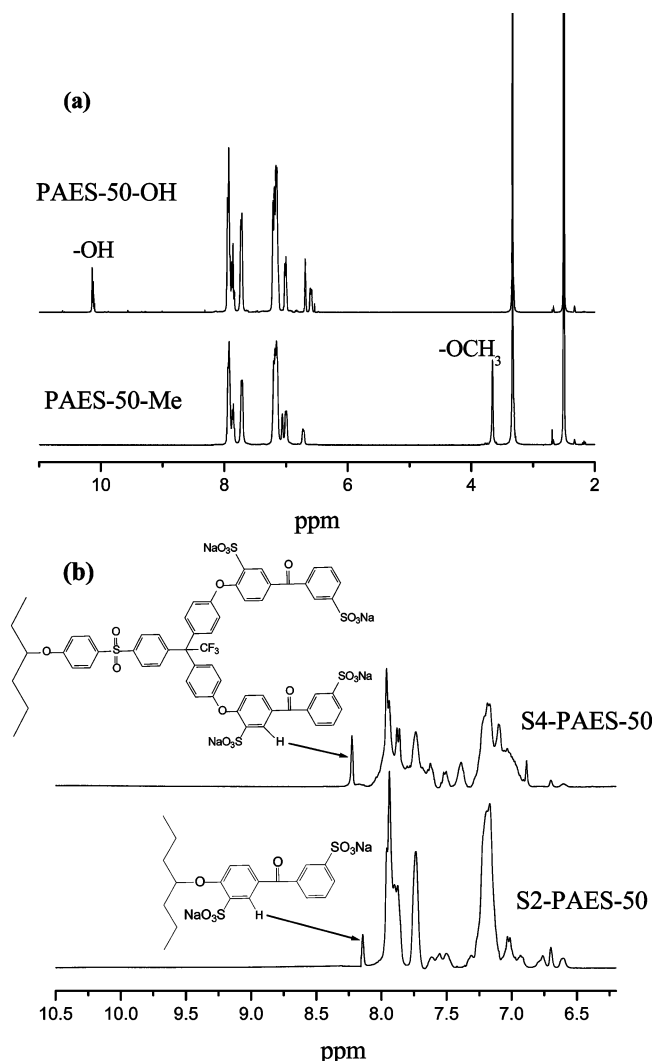


Figure 3. ^1H NMR of (a) PAES-50-Me, PAES-50-OH and (b) S2-PAES-50, S4-PAES-50.

fonated polymers in the dry state had tensile strength at maximum load in the range of 50–64 MPa, Young's modulus of 0.78–1.46 GPa, and elongation at break of 8.8–27%. In sulfonated polymers in the dry state, the S2-PAES-xx series membranes showed good mechanical properties with tensile stress of 40–49 MPa, Young's modulus of 0.88–1.3 GPa, and elongation at break of 8.3–10.5%. However, the S4-PAES-40, and -50 membranes showed inferior mechanical properties in dry state compared with the S2-PAES series. In the wet state, the sulfonated polymer showed tensile stress of 30–39 MPa, Young's modulus of 0.65–0.93 GPa, and elongation at break of 13.1–36%, which showed they were flexible materials. Compared to the data of Nafion with tensile stress of 28.4 MPa, Young's modulus of 0.1 GPa, and elongation at break of 329% in the wet state,¹⁸ these materials showed higher tensile strength and the lower elongation than Nafion.

Membrane Properties. Table 2 compares the density, ion exchange capacity (IEC), and water uptake of the sulfonated polymer (S2-PAES-xx, S4-PAES-xx) and Nafion 1135. The changes in length scale (reflected in volume measurements) are expected to be the most appropriate comparison basis because electrochemical properties such as proton conductivity and permeability occur over length scales under operating conditions independent of mass.² Still, dry weight-based measurements are most often quoted in the literature and appear in Table 2 for comparison purposes.

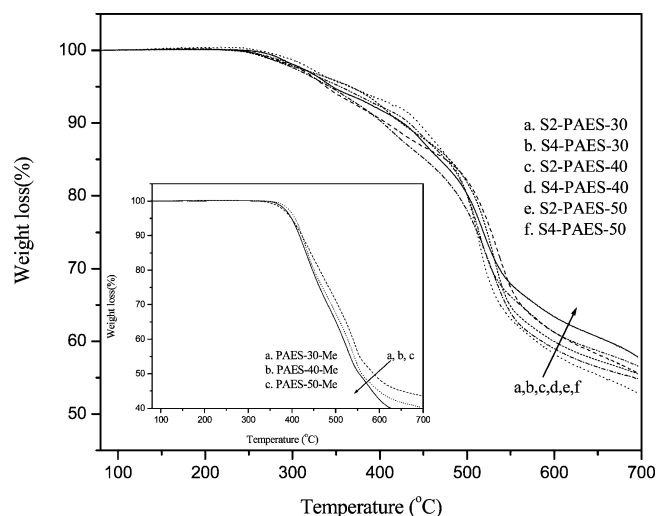


Figure 4. TGA curves of copolymers.

The water uptake directly affects the ion exchange capacity within the polymer matrix under hydrated conditions, which can be gauged by comparing wet volume based IEC (IEC_v (wet)) values with IEC_w values. Figure 5 shows a clear trend of increasing water uptake with IEC_w and IEC_v (dry). The volume-based data in Figure 5b showed the same trends as the weight based data in Figure 5a. The water uptake of S2-PAES-xx series increased linearly up to S2-PAES-50 ($\text{IEC}_w = 1.80$ mequiv/g, IEC_v (dry) = 2.29 mequiv/cm³) and then dramatically increased at S2-PAES-60, similar to that reported for other systems in the literature and related to a percolation threshold.⁴

The water uptake of S4-PAES-xx increased with IEC_w , IEC_v (dry), and IEC_v (wet). The IEC_v (wet) of S4-PAES-xx increased from 1.68 to 2.07 mequiv/cm³ as IEC_w changed from 1.62 to 2.0 mequiv/g. The IEC_v (wet) of S2-PAES-xx also increased from 1.31 to 1.65 mequiv/cm³ as IEC_w changed from 1.23 to 1.8 mequiv/g. However, the IEC_v (wet) of S2-PAES-60 was lower than that of other S2-PAES-xx. For S2-PAES-xx and S4-PAES-xx polymer, the increased sulfonic acid group concentration of the dry polymer was retained after equilibration with water, while hydration of S2-PAES-60 resulted in excessive swelling and dilution of the ion concentration after equilibration with water.² This is observed in Figure 5c whereby the slope of the 30 and 80 °C curves assumes a reverse direction due to high water uptake (vol %) and reduced IEC_v (wet). The trends in water uptake shown in Figure 5c are also seen in the plot of λ as a function of IEC_v (wet) (Figure 5d).

Kim² reported the IEC_v (wet) reflects the concentration of ions within the polymer matrix under hydrated conditions. Therefore, IEC_v (wet) was used as a basis for comparison in this study. Table 2 also shows the proton conductivity of sulfonated membranes and Nafion that were measured on free-standing membranes. The S2-PAES-50, -60 and S4-PAES-40, -50 had good conductivity (88–147 mS/cm) comparable to Nafion (125 mS/cm) at 80 °C. S2-PAES-40 and S4-PAES-30 showed moderate conductivity (51–63 mS/cm), and S2-PAES-30 had relatively low conductivity (34 mS/cm). Figure 6 shows the proton conductivity as a function of temperature. The proton conductivity increased with increasing temperature. The proton conductivities of S2-PAES-60 and S4-PAES-50 are higher than that of Nafion. Figure 7a shows the relative water uptake (vol %) as a function of relative proton conductivity. A high relative water uptake can lead to increased difficulties in MEA fabrication, membrane-electrode interfacial resistance, and membrane creep and deformation. Conductivity below 50 mS/cm can lead

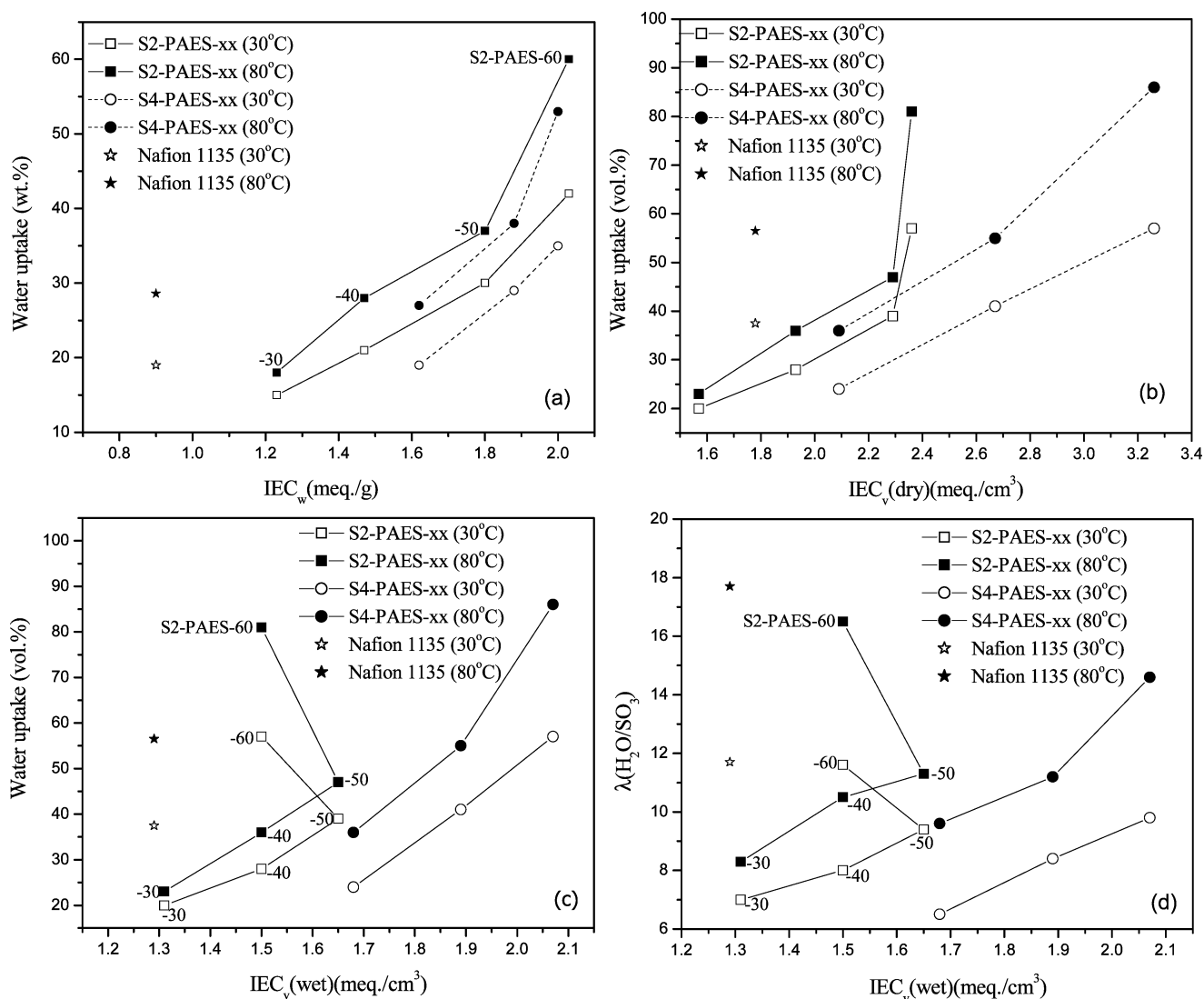


Figure 5. Water uptake as a function of (a) IEC_w , (b) $IEC_v(dry)$, (c) $IEC_v(wet)$, and (d) λ as a function of $IEC_v(wet)$.

Table 2. Properties of the Sx-PAES-yy Series and Nafion

copolymer	density ^a (g/cm ³)	IEC _w ^b (mequiv/g)	water uptake								rel selectivity ^f
			IEC _v ^c (mequiv/cm ³)		wt % ^d		vol % ^e		proton conductivity (mS/cm)		
			dry	wet	30 °C	80 °C	30 °C	80 °C	30 °C	80 °C	
S2-PAES-30	1.28	1.23	1.57	1.31	15	18	20	23	11	34	5.29
S2-PAES-40	1.31	1.47	1.93	1.50	21	28	28	36	15	51	4.90
S2-PAES-50	1.28	1.80	2.29	1.65	30	37	39	47	29	88	4.55
S2-PAES-60	1.35	2.03	2.36	1.50	42	60	57	81	85	147	2.99
S4-PAES-30	1.30	1.62	2.09	1.68	19	27	24	36	18	63	4.39
S4-PAES-40	1.45	1.88	2.67	1.89	29	38	41	55	31	96	2.45
S4-PAES-50	1.63	2.00	3.26	2.07	35	53	57	86	62	125	2.05
nafion 1135	1.98	0.90	1.78	1.29	19	28.6	37.5	56.5	57	125	1.00

^a Based on dry state. ^b Based on weight of dry membrane. ^c Based on volume of dry and/or wet membranes ($IEC_v(wet) = IEC_v(dry)/(1 + 0.01WU)$). ^d WU (mass %) = $(W_{wet} - W_{dry})/W_{dry} \times 100$. ^e WU (vol %) = $((W_{wet} - W_{dry})/\delta_w)/(W_{dry}/\delta_m) \times 100$ (W_{wet} and W_{dry} are the weights of the wet and dry membranes, respectively; δ_w is the density of water (g/cm³), and δ_m is the membrane density in the dry state.) ^f Relative selectivity = membrane selectivity/Nafion selectivity (selectivity = [proton conductivity]/[methanol permeability]) at 30 °C.

to significant ohmic losses under operation as minimum membrane thickness is often practically limited due to membrane fabrication or mechanical properties.²⁷ The methanol permeability through the proton exchange membranes often follows a similar relationship to proton conductivity. That is, the proton conductivity has a strong tradeoff in its relationship with the methanol permeability. Our target membrane would be located in the upper left-hand corner as shown in dotted circle, i.e.,

high conductivity and low methanol permeability. As shown in Figure 7b, S2-PAES-50 and S4-PAES-40 are located in this target area. Membranes intended for DMFC must both possess high proton conductivity and to be an effective barrier for methanol crossover from the anode to the cathode compartment. Nafion has good proton conductivity due to strongly interconnected ionic domains structure but also has high methanol permeability. Poly(arylene ether sulfone) containing sulfonated

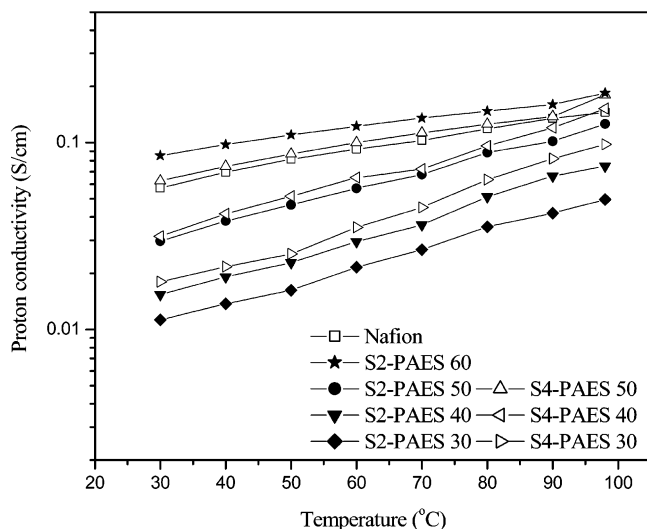


Figure 6. Proton conductivity as a function of temperature (°C).

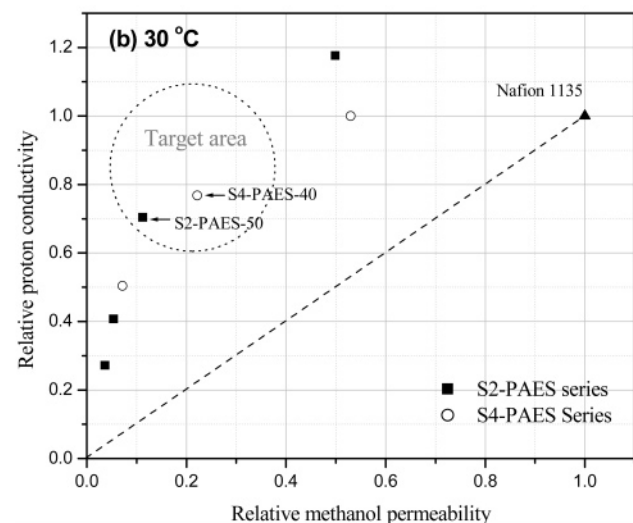
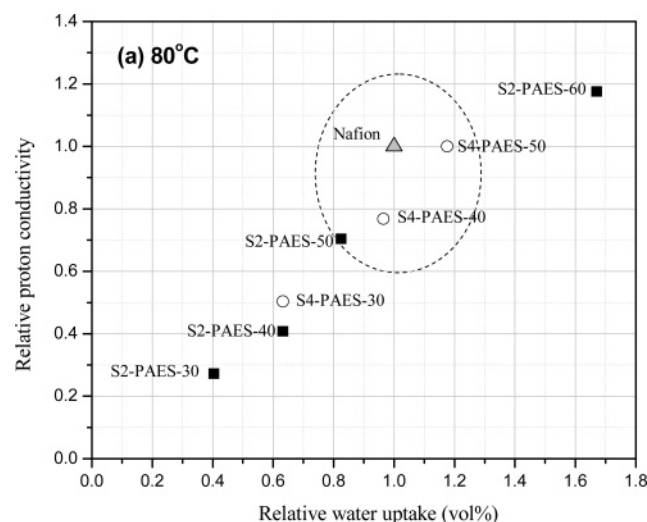


Figure 7. (a) Relative water uptake as a function of relative proton conductivity. (b) Relative proton conductivity as a function of relative methanol permeability.

monomer side chain exhibited extremely low methanol permeability. The methanol permeability values for 10% methanol concentration at room temperature were in the range of 5.66×10^{-8} – 7.73×10^{-7} cm²/s, which is several times lower than the value for Nafion of 1.55×10^{-6} cm²/s. Although S2-PAES

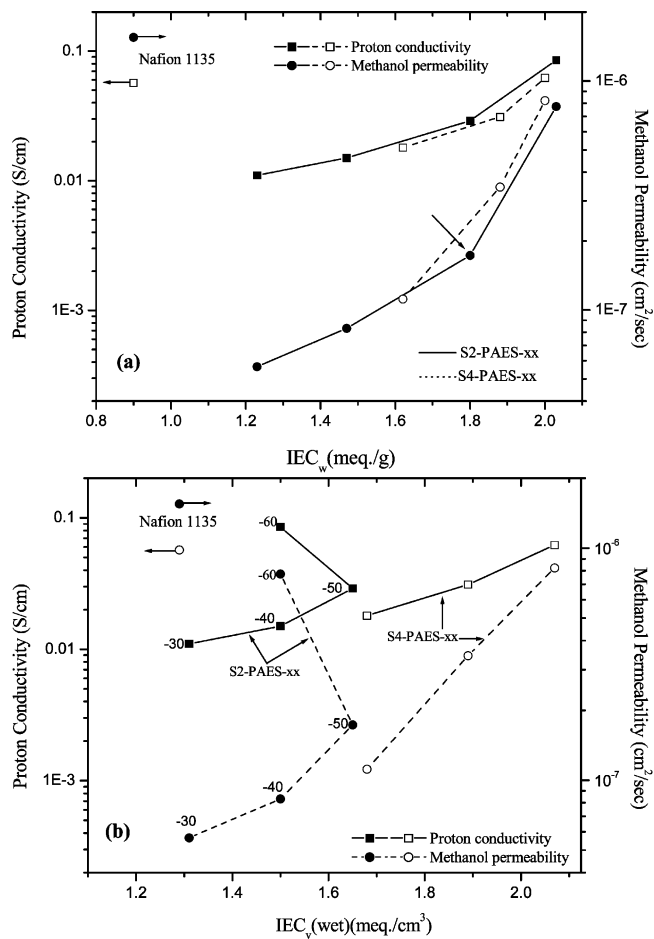


Figure 8. Proton conductivity and methanol permeability as a function of (a) IEC_w and (b) IEC_v (wet).

40 and S4-PAES 50 have lower cell proton conductivity than Nafion 1135, it is sufficient to achieve improved DMFC performance through its low methanol permeability (i.e., better selectivity) (target area in Figure 7b). The selectivity, which is the ratio of the proton conductivity to the methanol permeability, is often used to evaluate the potential performance of DMFC membranes.⁴ The relative selectivity of copolymers are higher than that of Nafion as listed in Table 2.

The proton conductivity and methanol permeability was plotted as a function of IEC_w (mequiv/g) and IEC_v(wet) (mequiv/cm³) in Figure 8. These data exhibit a deflection point at 1.80 mequiv/g where methanol permeability of S2-PAES-xx series increases substantially faster with IEC_w, similar to water uptake as shown in Figure 5, and related to a percolation threshold. In general, the introduction of a hydrophilic moiety enhances the water uptake, and also methanol molecules can pass through the hydrophilic domains. When IEC_w is changed to IEC_v(wet), the proton conductivities show the same trend as water uptake (vol %) shown in Figure 5c as shown in Figure 8b.

Proton conductivity and dimensional stability of the membranes are closely related to their morphology. Wide ion channels formed by hydrophilic domains are helpful to the movement of protons but are possibly detrimental for mechanical properties and dimensional stability in hot water.¹⁸ The microstructure of the S2-PAES-50 membrane was studied by TEM, as shown in Figure 9. The TEM suggests that the sulfonate groups might aggregate into hydrophilic clusters, appearing as the darkly stained spots in the copolymer matrix, which could provide proton transport pathways or ionic transport channels.²⁸ Assuming that the black clusters did not arise as an artifact from

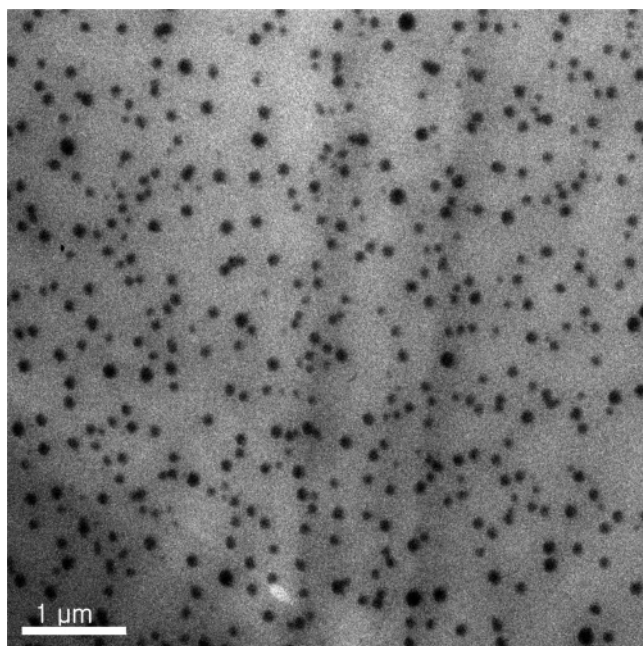


Figure 9. TEM photographs of S2-PAES-50.

sample preparation, it could be seen that the black clusters were randomly dispersed throughout the polymer matrix and that phase separation is not apparent. Similar TEM images have also previously been observed.²⁹ The dark regions most likely correspond to sulfonate groups with lead counterions and represent hydrophilic domains while the light regions correspond to hydrophobic regions. The black clusters are observed to be dispersed among the continuous area (hydrophobic domains).

Conclusions

New comb-shaped poly(arylene ether sulfone) copolymers having side chains containing 2 or 4 sulfonic acid groups have been prepared from commercially available monomers. The functionalized copolymers with graft side chains show thermal stability. The comb-shaped copolymers show high proton conductivities and low methanol permeabilities compared with Nafion membrane. S2-PAES-50 and S4-PAES-40 exhibited high proton conductivity of 88 and 96 mS/cm, respectively, at 80 °C. The methanol permeability values of S2-PAES-50 and S4-PAES-40 were 1.73×10^{-7} and 3.40×10^{-7} cm²/s, respectively, which is several times lower than Nafion. The combination of inexpensive monomers, high thermal stability, good relative proton and methanol transport, and relatively low water uptake makes S2-PAES-50 and S4-PAES-40 attractive as PEM materials for fuel cells applications.

Acknowledgment. The work was partially supported by the Technology and Innovation Fuel Cell Horizontal Program. TEM characterization by Mr. Dashan Wang of the National Research Council of Canada is gratefully acknowledged.

References and Notes

- (1) Hickner, M.; Ghassemi, H.; Kim, Y. S.; Einsla, B.; McGrath, J. E. *Chem. Rev.* **2004**, *104*, 4587.
- (2) Kim, Y. S.; Einsla, B.; Sankir, M.; Harrison, W.; Pivovar, B. S. *Polymer* **2006**, *47*, 4026.
- (3) Kerres, J. A. *J. Membr. Sci.* **2001**, *185*, 3.
- (4) Kim, D. S.; Shin, K. H.; Park, H. B.; Chung, Y. S.; Nam, S. Y.; Lee, Y. M. *J. Membr. Sci.* **2006**, *278*, 428.
- (5) Miyatake, K.; Chikashige, Y.; Watanabe, M. *Macromolecules* **2003**, *36*, 9691.
- (6) Fang, J. H.; Guo, X. X.; Harada, S.; Watari, T.; Tanaka, K.; Kita, H.; Okamoto, K. *Macromolecules* **2002**, *35*, 9022.
- (7) Miyatake, K.; Asano, N.; Watanabe, M. *J. Polym. Sci., Part A: Polym. Chem.* **2003**, *41*, 3901.
- (8) Genies, C.; Mercier, R.; Sillion, B.; Cornet, N.; Gebel, G.; Pineri, M. *Polymer* **2001**, *42*, 359.
- (9) Powers, E. J.; Serad, G. A. *High Performance Polymers: Their Origin and Development*; Elsevier: Amsterdam, 1986; p 355.
- (10) Wang, L.; Meng, Y. Z.; Wang, S. J.; Shang, X. Y.; Li, L.; Hay, A. S. *Macromolecules* **2004**, *37*, 3151.
- (11) Miyatake, K.; Oyaizu, K.; Tsuchida, E.; Hay, A. S. *Macromolecules* **2001**, *34*, 2065.
- (12) Kobayashi, T.; Rikukawa, M.; Sanui, K.; Ogata, N. *Solid State Ionics* **1998**, *106*, 219.
- (13) Ghassemi, H.; McGrath, J. E. *Polymer* **2004**, *45*, 5847.
- (14) Jones, D. J.; Rozière, J. *J. Membr. Sci.* **2001**, *185*, 41.
- (15) Gao, Y.; Robertson, G. P.; Guiver, M. D.; Mikhailenko, S. D.; Li, X.; Kaliaguine, S. *Macromolecules* **2005**, *38*, 3237.
- (16) Gao, Y.; Robertson, G. P.; Guiver, M. D.; Mikhailenko, S. D.; Li, X.; Kaliaguine, S. *Polymer* **2006**, *47*, 808.
- (17) Kim, D. S.; Robertson, G. P.; Guiver, M. D.; Lee, Y. M. *J. Membr. Sci.* **2006**, *281*, 111.
- (18) Liu, B.; Robertson, G. P.; Kim, D. S.; Guiver, M. D.; Hu, W.; Jiang, Z. *Macromolecules* **2007**, *40*, 1934.
- (19) Kreuer, K. D. *J. Membr. Sci.* **2001**, *185*, 29.
- (20) Einsla, B. R.; McGrath, J. E. *Am. Chem. Soc. Div. Fuel Chem.* **2004**, *49*, 616.
- (21) Ding, J.; Cuy, C.; Holdcroft, S. *Macromolecules* **2002**, *35*, 1348.
- (22) Lafitte, B.; Puchner, M.; Jannasch, P. *Macromol. Rapid Commun.* **2005**, *26*, 1464.
- (23) Norsten, T. B.; Guiver, M. D.; Murphy, J.; Astill, T.; Navesson, T.; Holdcroft, S.; Frankamp, B. L.; Rotello, V. M.; Ding, J. *Adv. Funct. Mater.* **2006**, *16*, 1814.
- (24) Li, Z.; Ding, J.; Robertson, G. P.; Guiver, M. D. *Macromolecules* **2006**, *39*, 6990.
- (25) Martinez, C. A.; Hay, A. S. *J. Polym. Sci., Part A: Polym. Chem.* **1997**, *35*, 2015.
- (26) Martinez, C. A.; Hay, A. S. *Polymer* **2002**, *43*, 3843.
- (27) Kim, Y. S.; Pivovar, B. S. In *Advances in Fuel Cells*; Zhao, T. S., Ed.; Elsevier: Oxford, 2007; Chapter 4.
- (28) Eisenberg, A. *Macromolecules* **1970**, *3*, 147.
- (29) Wang, Z.; Ni, H.; Zhao, C.; Li, X.; Zhang, G.; Shao, K.; Na, H. *J. Membr. Sci.* **2006**, *285*, 239.

MA7027215